

# Modified $z$ -gradient filtering as a mean to obtain phased deuterium autocorrelation 2D NMR spectra in oriented solvents

Olivier Lafon, Philippe Lesot\*, Denis Merlet, Jacques Courtieu

Laboratoire de Chimie Structurale Organique, CNRS UMR 8074, ICMMO, Université de Paris-Sud, Bât. 410, 91405 Orsay, France

Received 25 June 2004; revised 16 August 2004

Available online 17 September 2004

## Abstract

We describe a modified  $z$ -gradient filter scheme specifically designed to obtain pure absorption mode deuterium 2D NMR spectra recorded in oriented solvents. The proposed technique is investigated by analysing the evolution of the density operator for a spin  $I = 1$ . The method is applied to the recently designed  $Q$ -COSY and  $Q$ -resolved 2D experiments to simplify the analysis of chiral molecules dissolved in weakly orienting chiral liquid crystals. The efficiency of this  $z$ -gradient filtering technique is illustrated using the perdeuterated 1-butanol, a prochiral molecule of average  $C_s$  symmetry, dissolved in an organic solution of poly- $\gamma$ -benzyl-L-glutamate (PBLG). The experimental results as well as the advantages of the new experiments compared with the previous ones are described and discussed. © 2004 Elsevier Inc. All rights reserved.

**Keywords:**  $^2\text{H}$  NMR spectroscopy; Quadrupolar splittings; Chiral liquid crystals;  $z$ -Gradient filter

## 1. Introduction

Since a few years we are developing the use of deuterium NMR spectroscopy in chiral polypeptide liquid crystals as an original tool to study stereochemistry and chirality [1–3]. Among various 2D NMR techniques, we have shown that 2D  $Q$ -resolved ( $90_{(x)}^\circ-t_1/2-180_{(x)}^\circ-t_1/2-t_{2(x)}$ ) and  $Q$ -COSY ( $90_{(x)}^\circ-t_1-180_{(x)}^\circ-t_2(x)$ ) experiments are particularly efficient for simplifying the analysis of complex deuterium 1D spectra in perdeuterated materials [4,5]. Noticeably, these techniques are sufficiently sensitive to record deuterium NMR 2D spectra at natural abundance level [4,6–8]. Nevertheless, both of these techniques have inherently a major default because their 2D map cannot be phased due to the classical phase twist problem [9,10]. The reason is that the two sequences generate both a cosine and a sine term with respect to  $t_1$  after a single scan, leading to a sum

of absorption and dispersion signals after the double Fourier transform.

A  $Q$ -COSY Ph sequence designed to produce phased 2D deuterium spectra has also been described. This solution uses the “echo/antiecho” mode with both  $45^\circ$  and  $135^\circ$  reading pulses (instead of the  $180^\circ$  pulse) [4]. If resonances exhibit pure absorption mode in both dimensions, the 2D map obtained shows both deuterium autocorrelation peaks (off-diagonal) and diagonal peaks. The presence of the two types of signals is not useful and prevents the separation of the chemical shifts and the quadrupolar splittings as in case of the  $Q$ -resolved or  $Q$ -COSY experiments by applying the tilt procedure after the double Fourier transform [4]. More important is the significant loss of sensitivity observed for this sequence compared with the  $Q$ -COSY sequence (see Table 1). Such a situation is obviously not favourable for spectroscopic applications at deuterium natural abundance level (NAD). No attempt to produce  $Q$ -resolved experiment in phased mode was made so far.

In the first part of this contribution, we theoretically show that the above-mentioned experiments may be

\* Corresponding author. Fax: +33 0 1 69 15 81 05.

E-mail address: [philesot@icmo.u-psud.fr](mailto:philesot@icmo.u-psud.fr) (P. Lesot).

Table 1  
Comparative table of different 2D autocorrelation deuterium NMR experiments

Experiment features	<i>Q</i> -Resolved	<i>Q</i> -Resolved Fz	<i>Q</i> -COSY	<i>Q</i> -COSY Ph	<i>Q</i> -COSY Fz
<i>z</i> -Gradient filter	No	Yes	No	No	Yes
Minimum experiment number <sup>a</sup>	1	1 + 1	1	4 + 4	1 + 1
TPPI, State or State-TPPI procedure	No	Yes	No	Yes	Yes
Diagonal peaks	No	No	No	No <sup>d</sup>	No
Correlation peaks due to DD coupling	No	Yes	No	Yes	Yes
Tilt procedure	Yes	Yes	Yes	No	Yes
Symmetrization procedure	Yes <sup>b</sup>	Yes <sup>b</sup>	Yes	Yes	Yes
Relative signal amplitude prior to FT (1 scan)	1	3/4	1	1/4	2/3
Relative S/N ratio (eight scans) <sup>c</sup>	2	3/2	2	√2/2	4/3

<sup>a</sup> This number includes the TPPI (or States-TPPI) procedure when required.

<sup>b</sup> Symmetrization possible after the tilt procedure.

<sup>c</sup> S/N ratio is evaluated for an equivalent number of acquisitions (eight) and after the 2D Fourier transform. The relative S/N ratio of the 2D *Q*-resolved experiment is used as reference and is equal to 2.

<sup>d</sup> Echo-antiecho procedure.

performed in quadrature mode in both dimensions and without phase twist line shape through the simple addition to the initial sequence of a *z*-gradient filter with appropriate pulse angles and phases for spin  $I = 1$  nuclei. In the second part, the efficiency of *z*-gradient filtering is illustrated for deuterium using the perdeuterated 1-butanol (1) dissolved in an organic solution of poly- $\gamma$ -benzyl-L-glutamate (PBLG). The experimental results as well as the advantages of these 2D sequences compared with initial ones are reported and discussed.

## 2. Theoretical analysis

### 2.1. The *Q*-resolved experiment in phase mode

The deuterium *Q*-resolved sequence uses a classical spin echo during the  $t_1$  period of the 2D experiment, prior to the  $t_2$  acquisition of the signal [4]. During this echo, the deuterium chemical shift is refocused but not the quadrupolar splittings [9]. For spin-1 such as deuterium subjected only to chemical shift and quadrupolar interactions, the density operator at the end of the  $t_1$  evolution period,  $\rho(t_1)$  can be easily expressed as [9]:

$$\rho(t_1) = \begin{bmatrix} 0 & -i \frac{e^{-i(\pi q)t_1}}{\sqrt{2}} & 0 \\ i \frac{e^{+i(\pi q)t_1}}{\sqrt{2}} & 0 & -i \frac{e^{+i(\pi q)t_1}}{\sqrt{2}} \\ 0 & i \frac{e^{-i(\pi q)t_1}}{\sqrt{2}} & 0 \end{bmatrix} \quad (1)$$

where  $q$  is a half of the quadrupolar splitting expressed in Hertz.

At the end of the acquisition period,  $t_2$ , the density operator becomes:

$$\rho(t_1, t_2) = \begin{bmatrix} 0 & -i \frac{e^{-i(\pi q)t_1} e^{-i(\omega + \pi q)t_2}}{\sqrt{2}} & 0 \\ i \frac{e^{+i(\pi q)t_1} e^{+i(\omega + \pi q)t_2}}{\sqrt{2}} & 0 & -i \frac{e^{+i(\pi q)t_1} e^{-i(\omega - \pi q)t_2}}{\sqrt{2}} \\ 0 & i \frac{e^{-i(\pi q)t_1} e^{+i(\omega - \pi q)t_2}}{\sqrt{2}} & 0 \end{bmatrix} \quad (2)$$

with  $\omega = 2\pi\nu$ ,  $\nu$  is the resonance frequency of the spin  $I = 1$  nucleus.

The free induction decay,  $S(t_1, t_2)$ , can be determined through the expectation value  $\langle I^- \rangle$  of the in-phase ( $-1$ )-quantum coherence.  $S(t_1, t_2)$  is proportional to:

$$S(t_1, t_2) \propto \langle I^- \rangle = \text{Tr}[I^- \rho(t_1, t_2)] \\ = -ie^{-i(\pi q)t_1} e^{-i(\omega + \pi q)t_2} - ie^{+i(\pi q)t_1} e^{-i(\omega - \pi q)t_2}. \quad (3)$$

After a double Fourier transform, the two 2D peaks cannot be phased, as they are the sum of absorption and dispersion signals.

To find if there is a way to record phased spectra and quadrature in the  $F_1$  dimension, we explored the possibility to append just before the acquisition period of the *Q*-resolved sequence a *z*-gradient filter for storing part of the one-quantum coherences into *z*-magnetization. The use of *z*-filter, with gradient or not, was already used for spin 1/2 for different spectroscopic purposes but has never been applied for spin  $I = 1$  to the best of our knowledge [10,11]. The modified *z*-gradient filter developed for spin  $I = 1$  proceeds as shown in Fig. 1A. It is made of two identical hard pulses of angle  $\alpha$  and phase  $\phi$ , separated by a field gradient pulse parallel to the  $B_0$  axis (*z*-gradient) which is used to dephase all coherences. In this way the second  $\alpha$  pulse converts only the nuclear polarization created by the first  $\alpha$  pulse into coherences. The new *Q*-resolved sequence ( $90_{(x)}^{\circ} - t_1/2 - 180_{(x)}^{\circ} - t_1/2 - \alpha_{i(\phi)} - G_z - \alpha_{i(\phi)} - t_2(x)$  where  $i = 1$  (odd experiments) or 2 (even experiments)) is denoted “*Q*-resolved Fz” and the pulse diagram is displayed in Fig. 1B.

To understand the role of this *z*-gradient filter on a single spin  $I = 1$  nucleus, we have calculated its effect as a function of the pulse angle  $\alpha_1$  and phase  $\phi$  for the first experiment (odd). In the following calculations we only present the result when  $\phi = x$ . Applying a rotation of angle  $\alpha_1$  at the end of the  $t_1$  evolution period and then the  $G_z$  gradient yields the following density matrix:

$$\rho(t_1, G_z) = \begin{bmatrix} \sin(\alpha_1) \cos(\pi q t_1) & 0 & 0 \\ 0 & 0 & 0 \\ 0 & 0 & -\sin(\alpha_1) \cos(\pi q t_1) \end{bmatrix}. \quad (4)$$

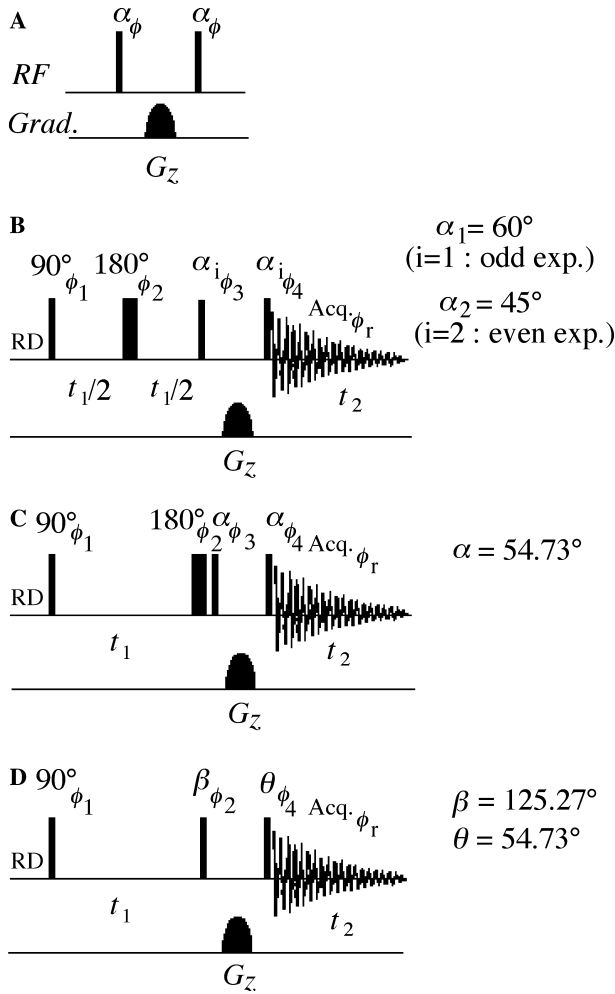


Fig. 1. (A) Schematic description of  $z$ -gradient filter applied for spin  $I = 1$ . The gradient pulse,  $G_z$ , suppresses all the coherences except the spin polarization and spin order term. The indice  $i$  for the  $\alpha$  pulse angle is used to separate the odd and even experiments (see text). (B) Pulse scheme of the 2D  $Q$ -resolved  $F_z$  experiment. The basic phase cycling is  $\phi_1 = 4(x)$ ;  $\phi_2 = x, y, -x, -y$ ;  $\phi_3 = \phi_4 = 4(x)$ ;  $\phi_r = 2(x, -x)$ . (C and D) Pulse scheme of the 2D  $Q$ -COSY  $F_z$  experiment including the  $z$ -gradient block and its three pulses variation. For the C and D sequences, the basic phase cycling is  $\phi_1 = 2(x)$ ;  $\phi_2 = \phi_3 = x, -x$ ;  $\phi_4 = 2(x)$ ;  $\phi_r = x, -x$ . In all sequences, the full phase cycling includes the CYCLOPS procedure. TPPI, States or States-TPPI method can be used to perform quadrature detection in  $F_1$  dimension.

At this stage, all coherences have been set to zero because they have been de-focussed by the  $z$ -gradient pulse and will not be re-focussed later. Consequently, this pulse stores along  $z$ -axis the cosine components of the one quantum coherences in Eq. (1), proportionally to  $\sin(\alpha_1)$ . In terms of product operator formalism it may be noted also that the density matrix,  $\rho(t_1, G_z)$ , is then proportional to  $I_z$  and corresponds to  $p = 0$  in the coherence transfer pathway. Now applying the second  $\alpha_{1(x)}$  pulse of the  $z$ -filter converts the spin polarization into one quantum coherences proportional to  $\sin^2(\alpha_1)$ :

$$\rho^+ = \begin{bmatrix} \frac{\sin(2\alpha_1)}{2} & i \frac{\sin^2(\alpha_1)}{\sqrt{2}} & 0 \\ -i \frac{\sin^2(\alpha_1)}{\sqrt{2}} & 0 & i \frac{\sin^2(\alpha_1)}{\sqrt{2}} \\ 0 & -i \frac{\sin^2(\alpha_1)}{\sqrt{2}} & -\frac{\sin(2\alpha_1)}{2} \end{bmatrix} \times \cos(\pi q t_1). \quad (5)$$

Applying the evolution operator during the detection period,  $t_2$ , the signal  $S(t_1, t_2)$  is then proportional to:

$$S(t_1, t_2) \propto \langle I^- \rangle = \sin^2(\alpha_1) \cos(\pi q t_1) i (e^{-i(\omega - \pi q)t_2} + e^{-i(\omega + \pi q)t_2}). \quad (6)$$

After a double Fourier transform, such a signal can be phased and the intensity will be maximum for  $\alpha_1 = \pi/2$ .

To be able to perform quadrature detection in the  $t_1$  dimension, the phase of the first two pulses can be incremented, thus leading to the sequence  $(90_{(y)}^{\circ})_{-t_1/2} - 180_{(y)}^{\circ} - t_1/2 - \alpha_{2(\phi)} - G_z - \alpha_{2(\phi)} - t_2$  (even experiments) and  $\phi = x$ . At the end of the spin echo sequence, the density operator is then:

$$\rho(t_1) = \begin{bmatrix} 0 & -\frac{e^{-i(\pi q)t_1}}{\sqrt{2}} & 0 \\ -\frac{e^{+i(\pi q)t_1}}{\sqrt{2}} & 0 & -\frac{e^{+i(\pi q)t_1}}{\sqrt{2}} \\ 0 & -\frac{e^{-i(\pi q)t_1}}{\sqrt{2}} & 0 \end{bmatrix}. \quad (7)$$

Applying the  $\alpha_{2(x)}$  pulses and the gradient yields:

$$\rho(t_1, G_z) = \begin{bmatrix} -\frac{1}{2} \sin(2\alpha_2) & 0 & 0 \\ 0 & +\sin(2\alpha_2) & 0 \\ 0 & 0 & -\frac{1}{2} \sin(2\alpha_2) \end{bmatrix} \times \sin(\pi q t_1). \quad (8)$$

Here, we store along  $z$ -axis the sine part of the coherences in Eq. (1), but this time the amplitude stored is proportional to  $\sin(2\alpha_2)$ , which is null for  $\alpha_2 = \pi/2$  and maximum for  $\alpha_2 = \pi/4$ . Furthermore, it must be noted that the density operator is not anymore proportional to the polarization  $I_z$  but to the spin order term  $(3I_z^2 - I^2)$  in the framework of the product operator formalism [9,10]. This change makes of course a tremendous difference. Let us anyway proceed and calculate the NMR signal in this situation. Applying the second pulse of the  $z$ -filter with the same phase  $\alpha_{2(x)}$  on Eq. (8) yields:

$$\rho^+ = \begin{bmatrix} -\frac{\{1+3\cos(2\alpha_2)\}\sin(2\alpha_2)}{8} & -i \frac{3\sin^2(2\alpha_2)}{4\sqrt{2}} & \frac{3\sin^3(\alpha_2)\cos(\alpha_2)}{2} \\ i \frac{3\sin^2(2\alpha_2)}{4\sqrt{2}} & \frac{\{1+3\cos(2\alpha_2)\}\sin(2\alpha_2)}{4} & i \frac{3\sin^2(2\alpha_2)}{4\sqrt{2}} \\ \frac{3\sin^3(\alpha_2)\cos(\alpha_2)}{2} & -i \frac{3\sin^2(2\alpha_2)}{4\sqrt{2}} & -\frac{\{1+3\cos(2\alpha_2)\}\sin(2\alpha_2)}{8} \end{bmatrix} \times \sin(\pi q t_1). \quad (9)$$

Applying now the evolution operator during  $t_2$  and calculating the expectation value of  $I^-$  yields the NMR signal  $S(t_1, t_2)$  equal to:

$$S(t_1, t_2) \propto \langle I^- \rangle = \frac{3\sin^2(2\alpha_2)}{4} \sin(\pi q t_1) i \times (e^{-i(\omega-\pi q)t_2} - e^{-i(\omega+\pi q)t_2}). \quad (10)$$

As expected, in this second experiment (even) we obtain the sine part of the signal in  $t_1$ . Unfortunately, the comparison with Eq. (6) shows that the signal amplitude for the odd and even experiments differ. This non-equivalence originates from the difference of behaviour of the polarization  $I_z$  and the spin order term ( $3I_z^2 - I^2$ ) under the effect of the second pulse in the  $z$ -filter. Such a situation is not correct to produce quadrature in  $F_1$  dimension using TPPI or States method [10]. To circumvent this problem we must determine a set of angles  $\alpha_1$  and  $\alpha_2$  that can provide the same intensity for odd and even experiments. Actually this condition is obtained when:

$$\sin^2(\alpha_1) = \frac{3\sin^2(2\alpha_2)}{4}. \quad (11)$$

Infinite pairs of  $\alpha_1$  and  $\alpha_2$  values can satisfy this equation, but the solutions are not equivalent in terms of signal amplitude. The signal reaches a maximum amplitude when  $\alpha_1 = 60^\circ$  and  $\alpha_2 = 45^\circ$ . For these specific angles each of the first (odd) and the second experiment (even) will have the same relative amplitude, namely 3/4. For odd and even experiments, the NMR signal,  $S(t_1, t_2)$ , can be written as:

$$\begin{aligned} \text{Experiment 1 (odd), } \alpha_1 &= 60^\circ \\ S(t_1, t_2) \propto \langle I^- \rangle &= \frac{3}{4} \cos(\pi q t_1) i (e^{-i(\omega-\pi q)t_2} + e^{-i(\omega+\pi q)t_2}). \\ \text{Experiment 2 (even), } \alpha_2 &= 45^\circ \\ S(t_1, t_2) \propto \langle I^- \rangle &= \frac{3}{4} \sin(\pi q t_1) i (e^{-i(\omega-\pi q)t_2} - e^{-i(\omega+\pi q)t_2}). \end{aligned} \quad (12)$$

Using this technique, it is possible to obtain a  $Q$ -resolved spectrum that can be phased in pure absorption mode and with quadrature detection in the  $F_1$  dimension. It must be noted that the same results are obtained incrementing the phase of the  $z$ -gradient filter instead of the phase of the two spin echo pulses.

## 2.2. The $Q$ -COSY experiment in phase mode

The same technique may be successfully applied to the 2D  $Q$ -COSY experiment where the entire echo is collected just after the  $180^\circ$  pulse during the acquisition period. The pulse sequence, denoted “ $Q$ -COSY Fz,” is reported in Fig. 1C. Doing the calculations in the same manner as above the following results are obtained. The NMR signal,  $S(t_1, t_2)$ , associated to the sequence  $(90_{(x)}^{\circ} t_1 180_{(x)}^{\circ} - \alpha_{(\phi)} - G_z - \alpha_{(\phi)} - t_{2(x)})$  where  $\phi = x$ ) is:

$$\begin{aligned} S(t_1, t_2) \propto \langle I^- \rangle &= \frac{1}{2} [\{1 + 3\cos^2(\alpha)\} \sin^2(\alpha)] [\cos(\omega - \pi q) t_1] \\ &\times i e^{-i(\omega+\pi q)t_2} + \frac{1}{2} [\{1 - 3\cos^2(\alpha)\} \sin^2(\alpha)] \\ &\times [\cos(\omega + \pi q) t_1] i e^{-i(\omega+\pi q)t_2} \\ &+ \frac{1}{2} [\{1 - 3\cos^2(\alpha)\} \sin^2(\alpha)] [\cos(\omega - \pi q) t_1] \\ &\times i e^{-i(\omega-\pi q)t_2} + \frac{1}{2} [\{1 + 3\cos^2(\alpha)\} \sin^2(\alpha)] \\ &\times [\cos(\omega + \pi q) t_1] i e^{-i(\omega-\pi q)t_2}. \end{aligned} \quad (13)$$

For the second experiment, the phase of the first  $90^\circ$  pulse is incremented by  $90^\circ$  and yields a signal,  $S(t_1, t_2)$ , equal to:

$$\begin{aligned} S(t_1, t_2) \propto \langle I^- \rangle &= -\frac{1}{2} [\{1 + 3\cos^2(\alpha)\} \sin^2(\alpha)] \\ &\times [\sin(\omega - \pi q) t_1] i e^{-i(\omega+\pi q)t_2} \\ &- \frac{1}{2} [\{1 - 3\cos^2(\alpha)\} \sin^2(\alpha)] \\ &\times [\sin(\omega + \pi q) t_1] i e^{-i(\omega+\pi q)t_2} \\ &- \frac{1}{2} [\{1 - 3\cos^2(\alpha)\} \sin^2(\alpha)] \\ &\times [\sin(\omega - \pi q) t_1] i e^{-i(\omega-\pi q)t_2} \\ &- \frac{1}{2} [\{1 + 3\cos^2(\alpha)\} \sin^2(\alpha)] \\ &\times [\sin(\omega + \pi q) t_1] i e^{-i(\omega-\pi q)t_2}. \end{aligned} \quad (14)$$

Here again, the 2D spectrum may be phased and quadrature is achievable using the TPPI procedure as it is possible to obtain alternatively the sine and cosine components in the  $t_1$  domain when incrementing the phase of the first pulse. Note here that contrarily to the  $Q$ -resolved Fz experiment, the increment of the phase of the first pulse does not modify the signal amplitude. This situation originates from the fact that the density operator associated with odd and even experiments is now a combination of  $I_z$  and ( $3I_z^2 - I^2$ ) terms during the  $z$ -gradient filter.

The NMR signal consists of autocorrelation peaks with intensities equal to  $I_{\text{auto}}(\alpha) = [\{1 + 3\cos^2(\alpha)\} \sin^2(\alpha)]/2$  and diagonal peaks with intensities equal to  $I_{\text{diag}}(\alpha) = [\{1 - 3\cos^2(\alpha)\} \sin^2(\alpha)]/2$ . As the main goal of this experiment is to correlate the two components of each quadrupolar doublet centred on a given chemical shift, we must maximise the intensity of the autocorrelation signals by optimising the  $\alpha$  angle. This angle corresponds to the value that nulls the derivative of  $I_{\text{auto}}(\alpha)$ . Such occurrence is obtained when  $\alpha$  is equal to the magic angle ( $\alpha = \theta_m = 54.73^\circ$ ) leading to  $I_{\text{auto}}(\theta_m) = 2/3$  as seen in Fig. 2. Advantageously, this angle corresponds also to the elimination of non-informative diagonal peaks in the 2D map, thus making possible the tilting of the 2D spectrum as in a  $Q$ -COSY experiment [4]. So using the “magic”  $z$ -gradient filter,  $\theta_m - G_z - \theta_m$ , allows for obtaining  $Q$ -COSY spectra with pure-phase lineshapes and quadrature detection in the  $F_1$  dimension. Here again, the same result is obtained when phases of the  $z$ -gradient are incremented.

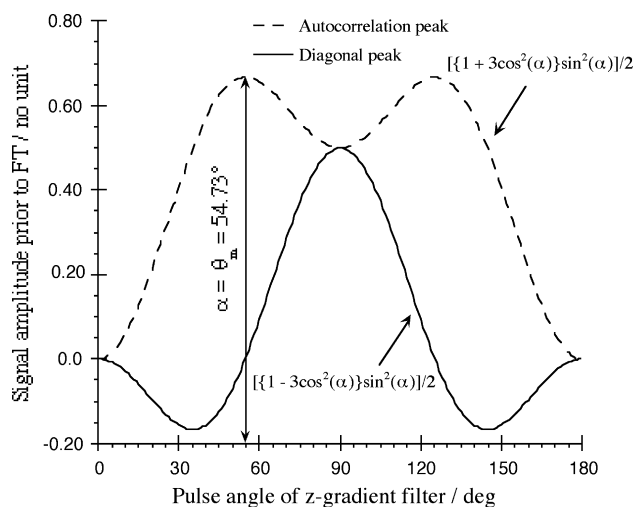


Fig. 2. Evolution of signal amplitude of autocorrelation and diagonal peaks as a function of the pulse angles of  $z$ -gradient filter for the 2D  $Q$ -COSY Fz sequence. At  $\alpha = \theta_m$ , the autocorrelation signal is maximum while the diagonal signal is eliminated.

A simple variation of the  $Q$ -COSY Fz experiment is possible by adding the  $180^\circ_x$  pulse and the first pulse,  $\alpha = \theta_m$ , of the  $z$ -gradient filter. This leads to a three-pulse sequence as shown in Fig. 1D. In this last sequence we use an angle of  $125.27^\circ$  as first pulse, corresponding to the complementary angle (i.e.,  $360^\circ - (180^\circ + 54.73^\circ)$ ) while keeping the second angle of the  $z$ -gradient filter equal to the magic angle.

### 3. Experimental

#### 3.1. Sample preparation

The NMR sample was prepared using 100 mg of PBLG with a DP = 1132, MW  $\approx$  248,000, (purchased from Sigma), 15 mg of perdeuterated 1-butanol, and 360 mg of dry chloroform. The components of the mixture were weighed into a 5 mm o.d. NMR tube which was sealed to avoid solvent evaporation. Other experimental details can be found in [2].

#### 3.2. NMR spectroscopy

The proton-decoupled deuterium experiments were performed on a Bruker DRX 400 high-resolution spectrometer equipped with a 5 mm diameter direct multinuclear probe operating at 61.4 MHz for deuterium. The NMR tubes were not spun along the magnetic field and the temperature was controlled by the Bruker BVT 3200 temperature unit. The sample temperature was regulated carefully at  $305.0 \pm 0.1$  K. In all deuterium spectra, the protons were broad-band decoupled using the WALTZ-16 sequence in order to remove possible proton-deuterium scalar and dipolar couplings

(isotopic enrichment  $<100\%$ ). All 2D spectra presented here were recorded using 0.9 s repetition time and 801 Hz spectral width in both dimensions. The spectral digitization was  $512(t_1) \times 1300(t_2)$  data points. The number of free induction decays added for each  $t_1$  increment was 16. Neither filtering in both dimensions prior to the double Fourier transformation nor symmetrization were used. The  $90^\circ$  deuterium pulse is set to 9.5  $\mu$ s. A sinus shape gradient pulse (24 G/cm) with length of 2 ms is used. Other experimental parameters are given in the figure captions.

### 4. Results and discussion

To experimentally explore and illustrate the potentialities of the  $Q$ -resolved Fz and  $Q$ -COSY Fz in the field of the enantiotopic and enantiomeric analysis, we investigate the case of **1** dissolved in the PBLG- $\text{CHCl}_3$  phase. This flexible prochiral molecule of average  $C_s$  symmetry possesses C–D enantiotopic directions in each methylene group that are in principle discriminated in chiral oriented solvents [12]. Consequently, we may a priori observe a maximum number of seven quadrupolar doublets corresponding to the various different inequivalent deuteriums including enantiotopic directions but disregarding the hydroxyl group.

Figs. 3B and C report the  $Q$ -resolved Fz and  $Q$ -resolved 2D spectrum of **1** recorded at 305 K. As expected, the first part of the sequence refocusses the deuterium chemical shifts in the  $F_1$  dimension and all signals can be phased on 2D  $Q$ -resolved Fz spectrum. Comparison between 2D maps and projections of both experiments clearly shows a significant gain in lineshape and resolution. Another benefit of the sequence is that magnetic field inhomogeneities are refocused during the  $t_1$  period, leading to narrower linewidths in the  $F_1$  dimension compared with linewidths in the  $F_2$  dimension. The tilt procedure allows to eliminate the quadrupolar splittings in the  $F_2$  dimension (2D spectrum not shown).

The analysis of the 2D map for **1** shows two different doublets corresponding to the *pro-R* and *pro-S* deuterons associated with the  $\alpha$  and  $\gamma$ -methylene but no spectral enantiodiscrimination is observed for the  $\beta$ -methylene group. Note the large enantiotopic discrimination (214 Hz) for the two deuterons on the methylene group attached to the hydroxyl group.

Figs. 3D and E report the three-pulse  $Q$ -COSY Fz and  $Q$ -COSY 2D spectrum of **1** recorded at 305 K. Contrary to the  $Q$ -resolved type experiments, both deuterium chemical shifts and quadrupolar doublets evolve during the  $t_1$  and  $t_2$  periods in the  $Q$ -COSY type experiments. Here again, deuterium signals in both dimensions can be phased after a double Fourier transform, and a significant gain in spectral resolution is obtained compared to the  $Q$ -COSY experiment. As diagonal

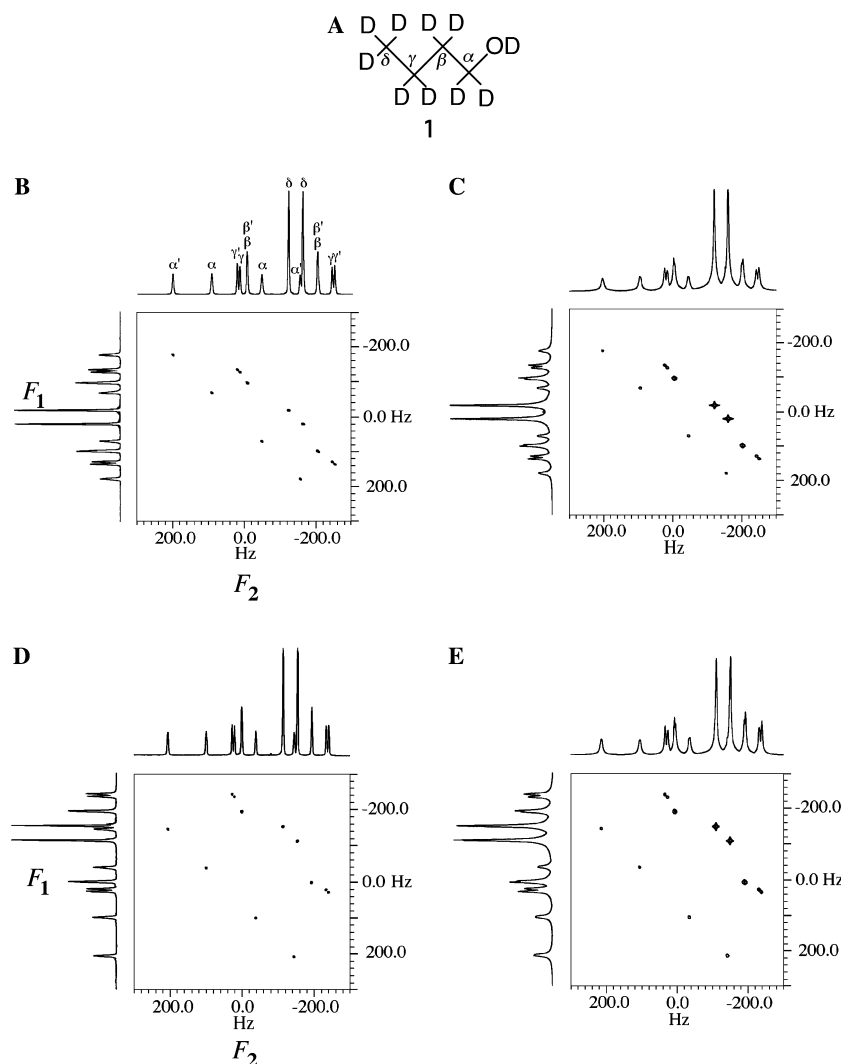


Fig. 3. (A) Structure and chemical notation of 1-butanol- $d_{10}$  (denoted **1**). (B and C) 61.4 MHz 2D spectra of **1** using the  $Q$ -resolved Fz and the classical  $Q$ -resolved sequence, respectively. (D and E) 61.4 MHz 2D map of **1** using the three-pulse  $Q$ -COSY Fz and the classical  $Q$ -COSY sequences, respectively. All 2D spectra have been recorded using the same experimental conditions. No filtering and no symmetrization were applied.

peaks are absent in the 2D  $Q$ -COSY Fz, it is possible to tilt the spectrum as in the  $Q$ -resolved 2D experiments (spectrum not shown). In this case, all the quadrupolar doublets line up parallel to the  $F_1$  axis [4]. This data manipulation produces a deuterium chemical shift spectrum in the  $F_2$  dimension (with a scaling factor of 2) and allows to extract the signal associated with all inequivalent deuterons on the basis of their chemical shift. This is an important advantage compared with the 2D  $Q$ -COSY Ph experiment where diagonal signals are present in the 2D map, thus preventing to apply the tilting procedure.

In Fig. 4 is shown the 2D  $Q$ -COSY Fz spectrum of **1** at very low contour level. Surprisingly, very low intensity extra peaks appear on the 2D map. Actually these small off-diagonal resonances correspond to the  $^2\text{H}$ - $^2\text{H}$  correlation signals between coupled deuterium atoms in the molecule ( $T_{\text{DD}} = J_{\text{DD}} + 2D_{\text{DD}}$ ). In this example,

$^2\text{H}$ - $^2\text{H}$  correlations between geminal deuterons of  $\alpha$ -methylene group are particularly well seen on the 2D spectrum due to the large separation of the quadrupolar doublets. The same type of signals should be observed for geminal deuterons of the  $\gamma$ -methylene group which are discriminated but peaks of interest are lost in the foot of autocorrelation resonances. At this very low contour level, some residual diagonal peaks which are not theoretically expected, appear because the pulses are not perfect. However due to their very low intensity, diagonal peaks are not a problem, and they might be removable by using appropriate composite pulses.

In the case of the 2D  $Q$ -COSY and  $Q$ -resolved experiments, it can be shown that  $^2\text{H}$ - $^2\text{H}$  correlation peaks cannot be observed. This occurrence is not true anymore for 2D  $Q$ -COSY Fz and 2D  $Q$ -resolved Fz experiments, and we can demonstrate that those correlations arise because the the  $z$ -gradient filter creates

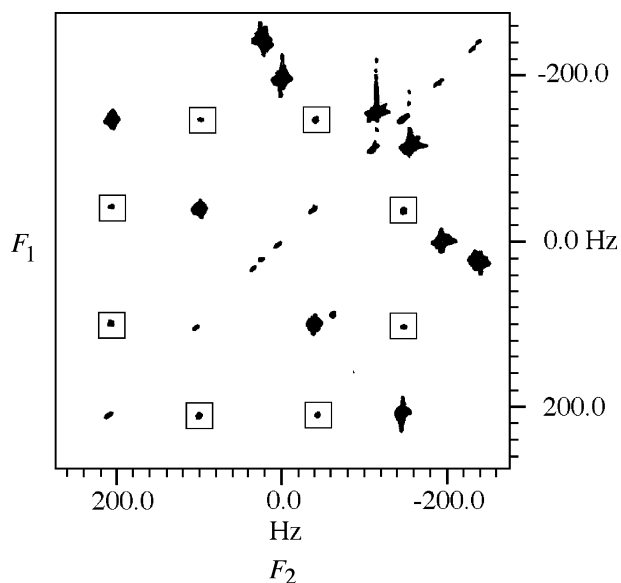


Fig. 4. 2D three-pulse  $Q$ -COSY Fz spectrum of **1** displayed at very low contour level (positive level). The intensity is multiplied by a factor of 8 compared with previous 2D contour plot. For such a level, we can see  $^2\text{H}$ - $^2\text{H}$  correlation peaks (showed by the squares) and some residual on-diagonal peaks.

multispin order terms,  $I_z S_z$ , in the case of two coupled deuterium nuclei [5]. The analysis of the spin operator evolution involving a pair of interacting deuteriums as well as numerical simulations using the NMRSIM module of the XWINNMR Bruker software have confirmed this result [5].

Thus, in the ideal case of two coupled non-equivalent deuterium nuclei (first-order system) for which all resonances are resolved (12 lines as shown in Fig. 5A), 68 resonances (36 components for autocorrelation peaks and 32 components for correlation peaks) are expected to be observed on the 2D  $Q$ -COSY Fz map as schematically displayed in Fig. 5B. In terms of peak intensity, the theoretical ratios (absolute value) between the various components of autocorrelation and correlation peaks, ( $I_{\text{auto}}/I_{\text{corr}}$ ), are equal to 6, 4, and 2, depending on their relative position in the 2D map. Experimentally, such spectral patterns are rarely observed because the extremely small magnitude of  $T_{\text{DD}}$  couplings measured in PBLG leads generally to non-resolved  $^2\text{H}$ - $^2\text{H}$  spectral patterns for correlation and autocorrelation signals.

Until now, only spin  $I=1$  COSY experiments ( $90_{(x)}^{\circ}-t_1-\alpha_{(x)}-t_2(x)$  with  $\alpha=90^{\circ}$  or  $45^{\circ}$ ) produced 2D spectra with  $^2\text{H}$ - $^2\text{H}$  correlation signals [5]. The presence of  $^2\text{H}$ - $^2\text{H}$  correlation signals can be efficiently used to confirm the assignment of quadrupolar doublets on the basis of their chemical shift. This spectral information can be also very advantageous for assigning the quadrupolar doublets of perdeuterated enantiomers dissolved in chiral oriented solvents for instance [5,13]. For compounds dissolved in the PBLG system, it is usual

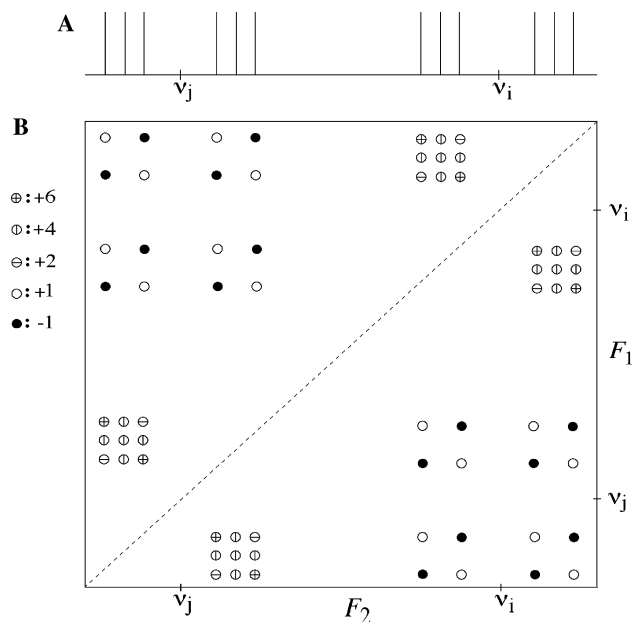


Fig. 5. (A) Schematic 1D  $^2\text{H}$  spectrum of two coupled non-equivalent deuteriums in an oriented solvent. The frequency of two nuclei,  $i$  and  $j$ , are labelled  $\nu_i$  and  $\nu_j$  with  $\nu_i \neq \nu_j$ . The quadrupolar doublet for each nucleus is assumed smaller than the frequency difference,  $\nu_i - \nu_j$ , but much larger than the total spin–spin coupling between  $i$  and  $j$ . (B) Schematic diagram of  $Q$ -COSY Fz 2D map for the same spin system. The relative intensity of all peaks (absorption lineshape) is indicated on the left part of the figure. Positive and negative peaks are labelled by open and solid circles, respectively.

that even the largest total spin–spin couplings, which are generally those between geminal deuterons, are not resolved.

#### 4.1. Possible applications in NAD NMR

In the field of the enantiotopic and enantiomeric analysis, deuterium NMR spectroscopy is the most interesting analytical tool, because quadrupolar interaction is the most sensitive anisotropic interaction to a difference of ordering generated by the chiral liquid crystalline phase. As isotopic labelling can be seen as a serious limitation of the method, we recently and successfully turned our attention to the NAD NMR spectroscopy in organic solutions of PBLG [6–8].

Due to the low abundance of deuterium at natural level, ( $1.5 \times 10^{-2}\%$ ), the sensitivity of any 2D experiments is an important point, and hence higher the sensitivity is, better the sequence for NAD NMR application is suitable.

In Table 1 is listed the main features of the  $Q$ -resolved and  $Q$ -COSY type experiments both in magnitude and phase mode, and in particular the S/N ratio for the same number of acquisitions (a total of eight) and after the double Fourier transform. As an evidence, the new 2D phase mode experiments proposed

here show a lower relative S/N ratio compared with the experiments performed in magnitude mode. However the  $Q$ -COSY Fz experiments are much more interesting than the  $Q$ -COSY Ph in terms of sensitivity (4/3 instead of  $\sqrt{2}/2$ ).

Although the S/N ratio for the  $Q$ -resolved Fz experiment is still smaller compared with the  $Q$ -resolved experiment, this latter provides the highest possible S/N ratio (3/2) when a  $z$ -gradient filter is used to generate pure absorption 2D spectrum, thus limiting the loss in sensitivity to only 25%. This experiment appears therefore the best compromise between an effectively improved resolution and the signal sensitivity.

## 5. Conclusions

In this work, we report a simple way to produce phased deuterium autocorrelation 2D NMR spectra in oriented solvents. To reach this aim, the addition of a modified  $z$ -gradient filter just before the acquisition period of the  $Q$ -resolved and  $Q$ -COSY experiments was explored and experimentally investigated. Disregarding the sensitivity problem, the new sequences proposed here lead to a significant gain in peak linewidth and resolution while the  $^2\text{H}$ - $^2\text{H}$  coupling information can be obtained without the need of new experiments. In addition in the case of the  $Q$ -COSY Fz experiments, the absence of diagonal peaks provides an interesting advantage in view to simplifying the analysis of the 2D maps after the tilt procedure as in the case of the  $Q$ -COSY. New solutions to obtain 2D phased maps without losing any sensitivity are currently being explored.

Although these new 2D experiments in phased mode are basically less sensitive than the experiments in magnitude mode, their use for NAD NMR applications should be suitable using spectrometers operating at higher field strengths or/and using a deuterium cryoprobe for which a significant gain in sensitivity will be obtained [8,14].

## Acknowledgment

The authors thank Prof. B. Ancian for his helpful discussions.

## References

- [1] I. Canet, J. Courtieu, A. Loewenstein, A. Meddour, J.-M. Péchiné, Enantiomeric analysis in a polypeptide lyotropic liquid crystal by deuterium NMR, *J. Am. Chem. Soc.* 117 (1995) 6520–6526.
- [2] M. Sarfati, P. Lesot, D. Merlet, J. Courtieu, Theoretical and experimental aspects of enantiomeric differentiation using natural abundance multinuclear NMR spectroscopy in polypeptide liquid crystals, *Chem. Commun.* (2000) 2069–2081 (and references therein).
- [3] C. Aroulanda, M. Sarfati, J. Courtieu, P. Lesot, Investigation of enantioselectivity of three polypeptide liquid-crystalline solvents using NMR spectroscopy, *Enantiomer* 6 (2001) 281–287.
- [4] D. Merlet, B. Ancian, J. Courtieu, P. Lesot, Two-dimensional deuterium NMR spectroscopy of chiral molecules oriented in a polypeptide liquid crystal: application for the enantiomeric analysis through natural abundance deuterium NMR, *J. Am. Chem. Soc.* 121 (1999) 5249–5258.
- [5] P. Lesot, M. Sarfati, D. Merlet, B. Ancian, J.W. Emsley, B.A. Timimi, 2D-NMR strategy dedicated to the analysis of perdeuterated enantiomer solutes in weakly ordered chiral liquid crystals, *J. Am. Chem. Soc.* 125 (2003) 7689–7695.
- [6] P. Lesot, D. Merlet, A. Loewenstein, J. Courtieu, Enantiomeric visualisation using proton-decoupled natural abundance deuterium in poly- $\gamma$ -benzyl-L-glutamate liquid crystalline solutions, *Tetrahedron: Asym.* 9 (1998) 1871–1881.
- [7] P. Lesot, M. Sarfati, D. Merlet, J. Courtieu, B. Ancian, C. Brevard, Determining enantiomeric purity NMR: deuterium 2D NMR at natural abundance in weakly oriented chiral liquid crystals, *Bruker Rep.* 149 (2001) 29–33.
- [8] P. Lesot, M. Sarfati, J. Courtieu, Natural abundance deuterium NMR spectroscopy in polypeptide liquid crystals as a new and incisive means for enantiodifferentiation of chiral hydrocarbons, *Chem. Eur. J.* 9 (2003) 1724–1745.
- [9] D. Merlet, B. Ancian, J. Courtieu, P. Lesot, Description of natural abundance deuterium 2D NMR experiments in weakly ordered liquid crystalline solvents using a tailored cartesian spin-operator formalism, *Phys. Chem. Chem. Phys.* 2 (2000) 2283–2290.
- [10] R.R. Ernst, G. Bodenhausen, A. Wokaun, *Principles of Nuclear Magnetic Resonance in One and Two Dimensions*, Clarendon Press, Oxford, 1987.
- [11] (a) O.W. Sorensen, M. Rance, R.R. Ernst, The  $z$ -filters for purging phase- or multiplet-distorted spectra, *J. Magn. Reson.* 56 (1984) 527–534;  
(b) E. Kupce, B. Wrackmeyer,  $Z$ -filtered heteronuclear polarization transfer, *J. Magn. Reson.* 99 (1992) 338–342;  
(c) G.A. Naganagowda, Use of  $B_0$  field gradients in one-dimensional NMR spectroscopy for spectral editing, *J. Magn. Reson. A* 113 (1995) 235–237;  
(d) K.E. Cano, M.J. Thrippleton, J. Keeler, A.J. Shaka, Cascaded  $z$ -filters for efficient single-scan suppression of zero-quantum coherence, *J. Magn. Reson.* 167 (2004) 291–297.
- [12] (a) A. Meddour, I. Canet, A. Loewenstein, J.-M. Péchiné, J. Courtieu, Observation of enantiomers, chiral by virtue of isotopic substitution, through deuterium NMR in a polypeptide liquid crystal, *J. Am. Chem. Soc.* 116 (1995) 9652–9656;  
(b) C. Aroulanda, D. Merlet, J. Courtieu, P. Lesot, NMR experimental evidence of the differentiation of enantiotopic directions in  $C_s$  and  $C_2$ , molecules using partially oriented, chiral media, *J. Am. Chem. Soc.* 123 (2001) 12059–12066.
- [13] J.W. Emsley, P. Lesot, D. Merlet, The orientational order and conformational distributions of the two enantiomers in a racemic mixture of a chiral, flexible molecule dissolved in a chiral nematic liquid crystalline solvent, *Phys. Chem. Chem. Phys.* 6 (2004) 522–530.
- [14] O. Lafon, P. Berdagué, P. Lesot, Use of two-dimensional correlation between  $^2\text{H}$  quadrupolar splittings and  $^{13}\text{C}$  CSA's for assignment of NMR spectra in chiral nematics, *Phys. Chem. Chem. Phys.* 6 (2004) 1080–1084.